

This article may be downloaded for personal use only. Any other use requires prior permission of the author and AIP Publishing.

The following article appeared in *Journal of Applied Physics* 117, 17C116 (2015); and may be found at <https://doi.org/10.1063/1.4915480>

## Magnetic entropy table-like shape in $RNi_2$ composites for cryogenic refrigeration

P. J. Ibarra-Gaytán, J. L. Sánchez Llamazares, Pablo Álvarez-Alonso, C. F. Sánchez-Valdés, Pedro Gorria, and J. A. Blanco

Citation: *Journal of Applied Physics* **117**, 17C116 (2015);

View online: <https://doi.org/10.1063/1.4915480>

View Table of Contents: <http://aip.scitation.org/toc/jap/117/17>

Published by the [American Institute of Physics](#)

---

### Articles you may be interested in

[Magnetocaloric properties of rapidly solidified  \$Dy\_3Co\$  alloy ribbons](#)

*Journal of Applied Physics* **117**, 17A706 (2015); 10.1063/1.4906764

[Magnetic entropy change and refrigerant capacity of rapidly solidified  \$TbNi\_2\$  alloy ribbons](#)

*Journal of Applied Physics* **113**, 17A912 (2013); 10.1063/1.4794988

[Texture-induced enhancement of the magnetocaloric response in melt-spun  \$DyNi\_2\$  ribbons](#)

*Applied Physics Letters* **103**, 152401 (2013); 10.1063/1.4824073

[Enhanced refrigerant capacity in Gd-Al-Co microwires with a biphasic nanocrystalline/amorphous structure](#)

*Applied Physics Letters* **108**, 092403 (2016); 10.1063/1.4943137

[Magnetostructural phase transitions and magnetocaloric effect in Tb-Dy-Ho-Co-Al alloys with a Laves phase structure](#)

*Journal of Applied Physics* **120**, 013901 (2016); 10.1063/1.4955047

[Observation of large low temperature magnetocaloric effect in  \$HoCu\_2\$](#)

*Journal of Applied Physics* **117**, 193904 (2015); 10.1063/1.4921360

---

**Scilight**

Sharp, quick summaries **illuminating**  
the latest physics research

Sign up for **FREE!**



## Magnetic entropy table-like shape in RNi<sub>2</sub> composites for cryogenic refrigeration

P. J. Ibarra-Gaytán,<sup>1</sup> J. L. Sánchez Llamazares,<sup>1</sup> Pablo Álvarez-Alonso,<sup>2</sup>  
 C. F. Sánchez-Valdés,<sup>1</sup> Pedro Gorria,<sup>3,a)</sup> and J. A. Blanco<sup>4</sup>

<sup>1</sup>Instituto Potosino de Investigación Científica y Tecnológica A.C., Camino a la Presa San José 2055 Col. Lomas 4a, San Luis Potosí, S.L.P. 78216, Mexico

<sup>2</sup>Departamento de Electricidad y Electrónica, UPV/EHU, 48940 Leioa, Spain

<sup>3</sup>Departamento de Física & IUTA, EPI, Universidad de Oviedo, 33203 Gijón, Spain

<sup>4</sup>Departamento de Física, Universidad de Oviedo, Calvo Sotelo st. s/n, 33007 Oviedo, Spain

(Presented 4 November 2014; received 22 September 2014; accepted 9 November 2014; published online 24 March 2015)

We have investigated the magnetocaloric (MC) effect in a two-phase composite based on melt-spun ribbons of the intermetallic DyNi<sub>2</sub> and TbNi<sub>2</sub> Laves phases. The temperature dependence of the isothermal magnetic entropy change,  $\Delta S_M(T)$ , has been calculated for the biphasic system  $x(\text{DyNi}_2) + y(\text{TbNi}_2)$  with  $0 < x < 1$  (i.e.,  $y = 1 - x$ ). The optimum MC properties, i.e., a  $\Delta S_M(T)$  curve with table-like shape, has been found in the temperature interval of 18–44 K for the composite with  $x = 0.4$  and for values of the magnetic field change  $\mu_0\Delta H = 2$  and 5 T, in good agreement with the experimental data. The refrigerant capacity,  $RC$ , reaches 221(526) J kg<sup>-1</sup> with a temperature span  $\delta T_{\text{FWHM}}$  of 32(41) K for  $\mu_0\Delta H$  of 2(5) T, thus improving the values obtained for the individual RNi<sub>2</sub> ribbons. Our findings constitute a good starting point to stimulate the search for new composites with enhanced MC properties at cryogenic temperatures. © 2015 AIP Publishing LLC.

[<http://dx.doi.org/10.1063/1.4915480>]

Magnetic refrigeration is an emerging cooling technology based on the magnetocaloric (MC) effect that is being developed in the wide range from room to low temperatures. In the latter, its main application is connected with the liquefaction of gases such as hydrogen and nitrogen.<sup>1</sup> In view of this, many investigations have been focused on the assessment of the MC properties of many rare earth-based RTX and RT<sub>2</sub> families (R = rare-earth metal, T = transition metal, and X = p-metal), owing to their large spontaneous magnetization and its rapid fall at the magnetic phase transition temperature, which may result in large values for the magnetic entropy change  $\Delta S_M$  within the cryogenic range.<sup>2–6</sup> Nevertheless, a MC material is attractive for magnetic refrigeration if sizeable  $\Delta S_M$  and adiabatic temperature change  $\Delta T_{\text{ad}}$  are combined with a large refrigerant capacity ( $RC$ ). This physical magnitude quantifies the amount of heat that can be extracted from the cold sink and transferred to the hot reservoir if an ideal refrigeration cycle is considered.<sup>7</sup>

Recently, it has been reported that melt-spun polycrystalline ribbons of the RNi<sub>2</sub> Laves phases with R = Tb and Dy may show enhanced  $RC$  values in comparison with their bulk counterparts produced by casting and prolonged high temperature annealing.<sup>8,9</sup> Actually, as  $RC$  basically depends on having a large peak value of the magnetic entropy change  $|\Delta S_M^{\text{peak}}|$  and a broad  $\Delta S_M(T)$  curve, it is difficult to increase beyond a certain limit for a single-phase material. A realistic approach to enhance  $RC$  is the fabrication of a two- or multi-phase MC material based on phases with a proper difference

in their magnetic transition temperatures. The latter leads to a decrease in the maximum value of the magnetic entropy change but expands the working temperature range of the resulting  $\Delta S_M(T)$  curve that is usually quantified by its full-width at half-maximum temperature span  $\delta T_{\text{FWHM}}$ . There are two types of composites, those obtained *in-situ* when the chemical composition, synthesis parameters and/or the processing method combine favorably to form a two-phase or multi-phase magnetic system<sup>10,11</sup> and those made of two amorphous melt-spun alloy ribbons in a proper weight fraction having an adequate difference in their  $T_C$  values and similar values of  $|\Delta S_M^{\text{peak}}|$ .<sup>12–15</sup> On the other hand, composites may also exhibit a table-like shaped  $\Delta S_M(T)$  curve, which is a desirable and pursuit attribute when the Ericsson-like magnetic refrigeration cycle is chosen.<sup>7</sup> Recently, Jeong reviewed Active Magnetic Regenerative (AMR) refrigeration technology for low temperature applications, underlying the importance in exploring layered composite structures with an extended operating temperature range.<sup>16</sup>

Motivated by these considerations, the aim of the present work is to investigate and optimize the MC effect in a two-ribbon composite system based on the intermetallic Laves phases DyNi<sub>2</sub> and TbNi<sub>2</sub>.

The melt-spun ribbons were fabricated from Argon arc-melted as-cast bulk ingots previously produced from highly pure elements (99.99% purity for Ni and 99.9% for Dy and Tb). The induction melted alloys were ejected through a circular nozzle of 0.5 mm in diameter onto the polished surface of a rotating copper wheel at a linear speed of 25 and 20 ms<sup>-1</sup> for DyNi<sub>2</sub> and TbNi<sub>2</sub>, respectively. The process was carried out under a highly pure Argon environment.

<sup>a)</sup>Author to whom correspondence should be addressed. Electronic mail: pgorria@uniovi.es

Magnetic measurements were performed by vibrating sample magnetometry in a Quantum Design PPMS<sup>®</sup> EverCool<sup>®</sup>-9 T platform. The magnetic field  $\mu_0 H$  was applied along the ribbon rolling direction in order to minimize the demagnetizing field effect. The magnetization as a function of temperature,  $M(T)$  curves, was recorded on cooling at 0.5 K/min under  $\mu_0 H = 5$  mT. The temperature dependencies of the magnetic entropy change  $\Delta S_M(T)$  were obtained by numerical integration of the Maxwell relation from a set of isothermal magnetization curves  $M(\mu_0 H)$  measured up to a maximum applied magnetic field of 5 T. The RC has been estimated from the  $\Delta S_M(T)$  curves assuming the three criteria used in the literature; they will be referred to as RC-1, RC-2, and RC-3 and their definition can be found in Ref. 17.

The typical low-field  $M(T)$  curves measured for DyNi<sub>2</sub> and TbNi<sub>2</sub> melt-spun ribbons are shown in Fig. 1(a); their Curie temperature values  $T_C$ , estimated as the minimum in the  $dM/dT$  vs.  $T$  curve, are 21.5 and 37 K, respectively. Thus, the Curie temperature difference  $\Delta T_C$  is 15.5 K. The total magnetic entropy change for the two ribbon composite  $\Delta S_M^{\text{comp}}(T)$  has been estimated from the calculated  $\Delta S_M(T)$  curves for the single DyNi<sub>2</sub> and TbNi<sub>2</sub> melt-spun ribbons [these are displayed in Figs. 2(a) and 2(b) for a magnetic field change  $\mu_0 \Delta H$  of 2 and 5 T, respectively]. A non-interacting field model with a rule-of-mixtures sum of the individual magnetic entropy change for different weight fraction values has been used (see Ref. 18 for further details).

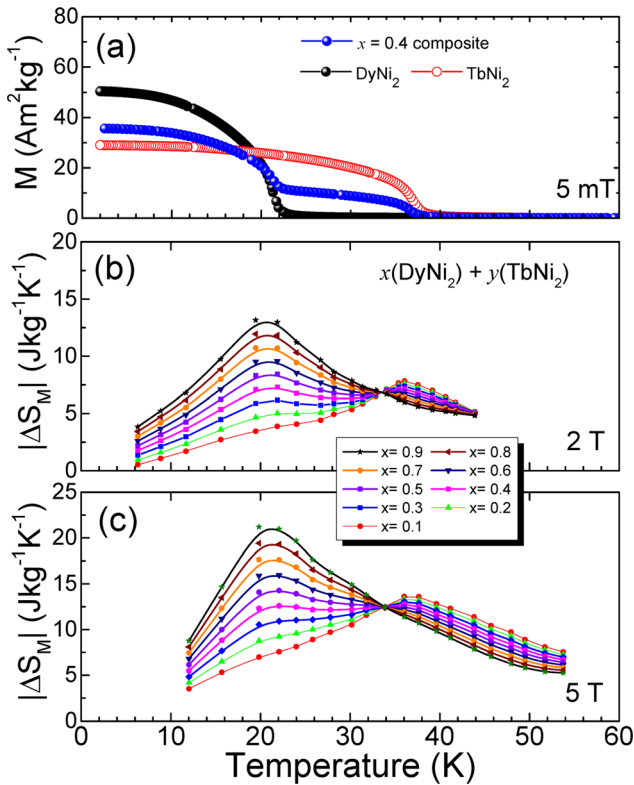


FIG. 1. (a) Temperature dependence of the magnetization measured under  $\mu_0 H = 5$  mT for DyNi<sub>2</sub> and TbNi<sub>2</sub> melt-spun ribbons together with that of the composite ( $x = 0.4$ ). (b) and (c) isothermal magnetic entropy change as a function of temperature calculated for a magnetic field change of 2 and 5 T, respectively, for the two-phase composite with  $0.1 \leq x \leq 0.9$  (see text for details). The lines are guides to the eye.

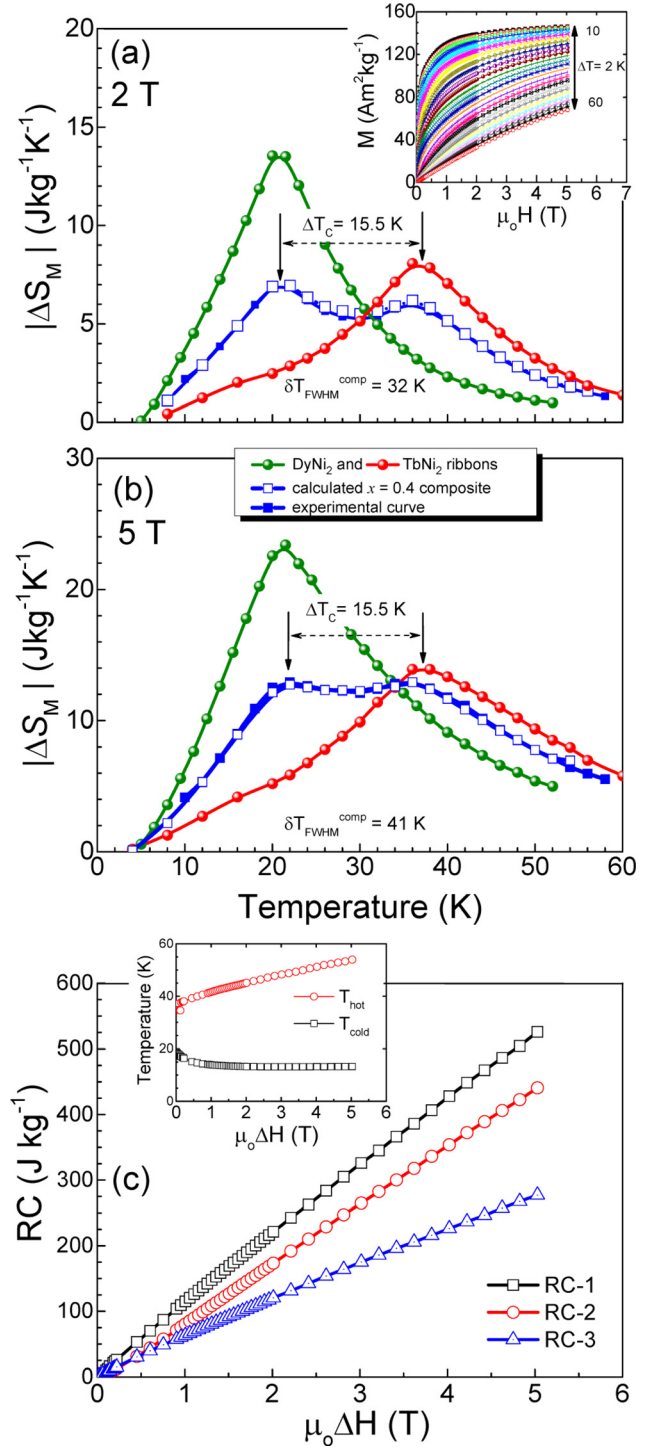


FIG. 2. Calculated and experimental  $\Delta S_M(T)$  curves of the composite with  $x = 0.4$  for  $\mu_0 \Delta H = 2$  T (a) and 5 T (b). The  $\Delta S_M(T)$  curves measured for melt-spun DyNi<sub>2</sub> and TbNi<sub>2</sub> alloy ribbons are also plotted for the sake of comparison. The inset in (a) shows the measured isothermal magnetization curves for the composite. (c) Refrigerant capacities RC-1, RC-2, and RC-3 as a function of  $\mu_0 \Delta H$  for the composite. Inset:  $T_{\text{hot}}$  and  $T_{\text{cold}}$  as a function of  $\mu_0 \Delta H$  for the composite.

The magnetic entropy change for the composite system  $x$  (DyNi<sub>2</sub>) +  $y$  (TbNi<sub>2</sub>) is given by

$$\Delta S_M^{\text{comp}}(T, \mu_0 \Delta H, x) = x \Delta S_M^{\text{DyNi}_2}(T, \mu_0 \Delta H) + y \Delta S_M^{\text{TbNi}_2}(T, \mu_0 \Delta H), \quad (1)$$

where  $x$  and  $y = 1 - x$  are the weight fraction of the DyNi<sub>2</sub> and TbNi<sub>2</sub> ribbons, respectively. In Figs. 1(b) and 1(c), we show the  $\Delta S_M^{\text{comp}}(T, x)$  curves (for  $\mu_0\Delta H = 2$  and 5 T, respectively) obtained following the above mentioned procedure [Eq. (1)]. As expected [see Fig. 1(b)], the curves exhibit a double-peak shape for  $x$  values between 0.3 and 0.7 in the case of  $\mu_0\Delta H = 2$  T. This feature results from the particular shape of the  $\Delta S_M(T)$  curves and the value of  $\Delta T_C$ , as already observed in other composites.<sup>12,14</sup> The position of the peaks coincides with the value of  $T_C$  for the single ribbons (i.e., 21.5 and 37 K). However, the difference in height between these two peaks diminishes as the magnetic field change increases from 2 T up to 5 T [see Fig. 1(c)]. Interestingly, the  $\Delta S_M^{\text{comp}}(T, x)$  curve for the composite with  $x = 0.4$  shows an almost flat or table-like shape for  $\mu_0\Delta H = 5$  T [between  $T = 18$  and 44 K, see Fig. 1(b)]. Therefore, we have selected  $x = 0.4$  to prepare and characterize a two-phase composite. It consists of two stuck ribbons wrapped between two Kapton<sup>®</sup> adhesive films with the following approximate dimensions: 4 mm (long), and 1 mm (wide). The experimental  $M(T)$  curve measured under low applied magnetic field (5 mT) exhibits the expected two-step behavior [see Fig. 1(a)]. From the set of isothermal magnetization curves,  $M(H)$ , shown in the inset of Fig. 2(a) (measured from 10 to 60 K in  $\Delta T$  steps of 2 K), we have obtained the  $\Delta S_M^{\text{comp}}(T)$  curves.

The  $\Delta S_M(T)$  curves for the constituent ribbons as well as the  $\Delta S_M^{\text{comp}}(T)$  curve for the composite with  $x = 0.4$  [the one calculated using Eq. (1) and that obtained from experimental  $M(H)$  data] are depicted in Figs. 2(a) and 2(b) for  $\mu_0\Delta H = 2$  and 5 T, respectively. It is worth noting the excellent agreement between both  $\Delta S_M^{\text{comp}}(T)$  curves. As foreseen by the calculation,  $|\Delta S_M|$  remains almost constant between 18 and 44 K, and its value is comparable to that of  $|\Delta S_M^{\text{peak}}|$  for the TbNi<sub>2</sub> ribbon. Fig. 2(c) evidences that the refrigerant capacity, whatever the calculation method is employed ( $RC-1$ ,  $RC-2$ , or  $RC-3$ ), displays a quasi-linear dependence upon the magnetic field change up to 5 T. Table I summarizes the MC properties of the composite. Note that the

TABLE I. Values of the peak of the magnetic entropy change  $|\Delta S_M^{\text{peak}}|$ ,  $RC-1$ ,  $RC-2$ ,  $\delta T_{\text{FWHM}}$ ,  $T_{\text{hot}}$ ,  $T_{\text{cold}}$ ,  $RC-3$ ,  $\delta T^{\text{RC-3}}$ , and  $T_{\text{hot}}$  and  $T_{\text{cold}}$  related to  $RC-3$  for the composite with  $x = 0.4$ .

	$\mu_0\Delta H$	
	2 T	5 T
$ \Delta S_M^{\text{peak}} $ (J kg <sup>-1</sup> K <sup>-1</sup> )	6.9	12.9
$RC-1$ (J kg <sup>-1</sup> )	221	526
$RC-2$ (J kg <sup>-1</sup> )	173	441
$\delta T_{\text{FWHM}}$ (K)	32	41
$T_{\text{hot}}$ (K)	45	54
$T_{\text{cold}}$ (K)	13	13
$RC-3$	121	277
$\delta T^{\text{RC-3}}$ (K)	25	32
$T_{\text{hot}}^{\text{RC-3}}$ (K) <sup>a</sup>	41	48
$T_{\text{cold}}^{\text{RC-3}}$ (K) <sup>a</sup>	16	16

<sup>a</sup>Related to  $RC-3$ .

values of  $\delta T_{\text{FWHM}}$  and  $RC-1$ ,  $RC-2$ , and  $RC-3$  are enhanced with respect to the individual ribbons. Indeed,  $\delta T_{\text{FWHM}}$  is 2.0 and 1.5 times larger than the values found in DyNi<sub>2</sub> and TbNi<sub>2</sub>, respectively. The inset in Fig. 2(c) shows how the values of  $T_{\text{hot}}$  and  $T_{\text{cold}}$  evolve as  $\mu_0\Delta H$  is increased (i.e.,  $\delta T_{\text{FWHM}} = T_{\text{hot}} - T_{\text{cold}} = 32$  and 41 K for  $\mu_0\Delta H = 2$  and 5 T, respectively). Finally, Table II compares the main MC properties of the  $x = 0.4$  composite with those corresponding with the single ribbons and with those reported for other materials with a transition temperature below 40 K,<sup>4,5,8-10,19-24</sup> the largest values of  $\delta T_{\text{FWHM}}$  being those found for the composite. Moreover, the value for  $RC-1$  is higher than those of single DyNi<sub>2</sub> and TbNi<sub>2</sub> melt-spun ribbons and close to those reported for the bulk alloys Er<sub>0.2</sub>Tb<sub>0.8</sub>Al<sub>2</sub>, DyCoAl, and DyCuAl.<sup>4,19,20</sup>

It is noteworthy that the shape and behavior of the extensive entropy change  $\Delta S_M(T)$  curves can vary notoriously from one material to another. In particular, for

TABLE II. Transition temperature ( $T_{\text{trans}}$ ), peak value of the magnetic entropy change  $|\Delta S_M^{\text{peak}}|$ , refrigerant capacity  $RC-1$ , and  $\delta T_{\text{FWHM}}$  for the composite with  $x = 0.4$ . For the sake of comparison data for RNi<sub>2</sub> (R = Dy and Tb) melt-spun ribbons and other materials with  $20 < T_{\text{trans}} < 40$  K are included.

Material	$T_{\text{trans}}$ (K)	$ \Delta S_M^{\text{peak}} $ (J kg <sup>-1</sup> K <sup>-1</sup> )		$RC-1$ (J kg <sup>-1</sup> )		$\delta T_{\text{FWHM}}$ (K)		Transition type	References
		2 T	5 T	2 T	5 T	2 T	5 T		
$x = 0.4$ composite	...	6.9	12.9	221	526	32	41	FM-PM	This work
DyNi <sub>2</sub> ribbons	21.5	13.5	23.5	209	519	16	23	FM-PM	8
TbNi <sub>2</sub> ribbons	37.0	8.0	13.9	166	441	20	32	FM-PM	9
Er <sub>0.8</sub> Tb <sub>0.2</sub> Al <sub>2</sub> <sup>a</sup>	27	8.6	18.8	253	666	29	36	FM-PM	19
DyCoAl <sup>a</sup>	37	9.2	16.3	234	616	26	38	FM-PM	5
DyCuAl <sup>a</sup>	28	10.9	20.4	190	566	17	28	FM-PM	20
GdCo <sub>2</sub> B <sub>2</sub> <sup>a</sup>	25	9.4	17.2	166	474	14	27	AFM-FM	21
Ho <sub>3</sub> Ni <sub>2</sub> <sup>a</sup>	33	9.8	21.6	162	485	16	22	FM-PM	10
DyNi <sub>2</sub> <sup>a</sup>	21	10.7	21.1	140	443	13	20	FM-PM	4
TbCoC <sub>2</sub> <sup>a</sup>	28	7.8	15.3	114	379	14	25	FM-PM	22
ErCo <sub>2</sub> <sup>a</sup>	35	...	33.0	...	332	...	11	AFM-FM	23
NdMn <sub>2</sub> Ge <sub>0.4</sub> Si <sub>1.6</sub> <sup>a</sup>	36	12.3	18.4	91	274	7	14	AFM-FM	24

<sup>a</sup>Bulk alloy.

materials undergoing a second-order magnetic phase transition (such as those  $\text{RNi}_2$ )  $\Delta S_M(T)$  curve is often characterized by a broad caret-like peak.<sup>2-4</sup> The position is mainly determined by the exchange interactions and appears to be located in the vicinity of the magnetic ordering temperature.<sup>3,4,6</sup> The use of a composite constituted of two dissimilar materials with different but close magnetic ordering temperatures could improve the magnetocaloric effect of the whole system [such as  $x(\text{DyNi}_2) + y(\text{TbNi}_2)$ ], leading to a table-like shape for the magnetic entropy. In the present case,  $|\Delta S_M^{\text{peak}}|$  has a larger magnitude for  $\text{DyNi}_2$  than for  $\text{TbNi}_2$ , while the opposite ensues for  $\delta T_{\text{FWHM}}$ . Then, the balanced entropy changes for having an almost flat  $\Delta S_M(T)$  curve corresponds to the case  $x=0.4$ , which slightly reduces the influence of  $\text{DyNi}_2$  compared to  $\text{TbNi}_2$ . However, an enhancement of the magnetocaloric effect can be also achieved by considering multiple transitions, provided that the magnetic ordering temperatures and  $\Delta S_M(T)$  shape were appropriated, even in a single material (polycrystalline, nanostructured, or amorphous), as recently reported in the  $\text{R}_2\text{Fe}_{17}$  system.<sup>25,26</sup>

In summary, we report on the MC effect in the two-ribbon composite system  $x(\text{DyNi}_2) + y(\text{TbNi}_2)$  with  $0 < x < 1$ . We observe that the optimum MC behavior, i.e., a table-like shape in the  $\Delta S_M(T)$  curve, occurs for  $x=0.4$  and appears for  $\mu_0\Delta H = 5$  T within the temperature interval from 18 to 44 K. The maximum value of the isothermal magnetic entropy change,  $|\Delta S_M^{\text{peak}}| = 12.9$  (6.9)  $\text{J kg}^{-1} \text{K}^{-1}$  for  $\mu_0\Delta H = 5$  (2) T is close to that of the  $\text{TbNi}_2$ . In addition, the broadening of the  $\Delta S_M(T)$  curve provokes an enhancement of the refrigerant capacity reaching values comparable to those reported for materials with first- and second-order magnetic phase transitions below 40 K. These findings make this composite material competitive as magnetic refrigerant at cryogenic temperatures.

This work was financially supported by (a) Projects CB-2010-01-156932 (CONACyT, Mexico), MAT2011-27573-C04 (MINECO, Spain), and IT711-13 (Basque Government, Spain); (b) Laboratorio Nacional de Investigaciones en Nanociencias y Nanotecnología (LINAN, IPICYT). C. F. Sánchez-Valdés thanks LINAN, IPICYT, and CONACyT (Project No. CB-2012-01-183770), for supporting his postdoctoral stay. P. J. Ibarra-Gaytán thanks CONACyT for

the Ph.D. grant received and also IPICYT for supporting his stay, Mexico.

- <sup>1</sup>K. A. Gschneidner, Jr., H. Takeya, J. O. Moorman, and V. K. Pecharsky, *Appl. Phys. Lett.* **64**, 253 (1994).
- <sup>2</sup>K. A. Gschneidner, Jr., V. K. Pecharsky, and A. O. Tsokol, *Rep. Prog. Phys.* **68**, 1479 (2005).
- <sup>3</sup>N. A. de Oliveira and P. J. von Ranke, *Phys. Rep.* **489**, 89 (2010).
- <sup>4</sup>P. J. von Ranke, V. K. Pecharsky, and K. A. Gschneidner, Jr., *Phys. Rev. B* **58**, 12110 (1998).
- <sup>5</sup>X. X. Zhang, F. W. Wang, and G. H. Wen, *J. Phys.: Condens. Matter* **13**, L747 (2001).
- <sup>6</sup>P. Alvarez, P. Gorria, and J. A. Blanco, *Phys. Rev. B* **84**, 024412 (2011).
- <sup>7</sup>M. E. Wood and W. H. Potter, *Cryogenics* **25**, 667 (1985).
- <sup>8</sup>P. J. Ibarra-Gaytán, C. F. Sánchez-Valdés, J. L. Sánchez Llamazares, P. Álvarez-Alonso, P. Gorria, and J. A. Blanco, *Appl. Phys. Lett.* **103**, 152401 (2013).
- <sup>9</sup>J. L. Sánchez Llamazares, C. F. Sánchez-Valdés, P. J. Ibarra-Gaytán, P. Álvarez-Alonso, P. Gorria, and J. A. Blanco, *J. Appl. Phys.* **113**, 17A912 (2013).
- <sup>10</sup>Q. Y. Dong, J. Chen, J. Shen, J. R. Sun, and B. G. Shen, *Appl. Phys. Lett.* **99**, 132504 (2011).
- <sup>11</sup>H. Fu, Z. Ma, X. J. Zhang, D. H. Wang, and B. H. Teng, *Appl. Phys. Lett.* **104**, 072401 (2014).
- <sup>12</sup>P. Álvarez, J. L. Sánchez Llamazares, P. Gorria, and J. A. Blanco, *Appl. Phys. Lett.* **99**, 232501 (2011).
- <sup>13</sup>A. M. Aliev, A. G. Gamzatov, K. I. Kamilov, A. R. Kaul, and N. A. Babushkina, *Appl. Phys. Lett.* **101**, 172401 (2012).
- <sup>14</sup>S. C. Paticopoulos, R. Caballero-Flores, V. Franco, J. S. Blázquez, A. Conde, K. E. Knipling, and M. A. Willard, *Solid State Commun.* **152**, 1590 (2012).
- <sup>15</sup>J. J. Wang, Z. D. Han, Q. Tao, B. Qian, P. Zhang, and X. F. Jiang, *Physica B* **416**, 76 (2013).
- <sup>16</sup>S. Jeong, *Cryogenics* **62**, 193 (2014).
- <sup>17</sup>P. Gorria, J. L. Sánchez Llamazares, P. Álvarez, M. J. Pérez, J. Sánchez Marcos, and J. A. Blanco, *J. Phys. D: Appl. Phys.* **41**, 192003 (2008).
- <sup>18</sup>P. Álvarez, P. Gorria, J. L. Sánchez Llamazares, and J. A. Blanco, *J. Alloys Compd.* **568**, 98 (2013).
- <sup>19</sup>M. Khan, K. A. Gschneidner, Jr., and V. K. Pecharsky, *J. Appl. Phys.* **107**, 09A904 (2010).
- <sup>20</sup>Q. Y. Dong, B. G. Shen, J. Chen, J. Shen, and J. R. Sun, *J. Appl. Phys.* **105**, 113902 (2009).
- <sup>21</sup>L. Li, K. Nishimura, and H. Yamane, *Appl. Phys. Lett.* **94**, 102509 (2009).
- <sup>22</sup>B. Li, W. J. Hu, X. G. Liu, F. Yang, W. J. Ren, X. G. Zhao, and Z. D. Zhang, *Appl. Phys. Lett.* **92**, 242508 (2008).
- <sup>23</sup>N. K. Singh, K. G. Suresh, A. K. Nigam, S. K. Malik, A. A. Coelho, and S. Gama, *J. Magn. Magn. Mater.* **317**, 68 (2007).
- <sup>24</sup>J. L. Wang, S. J. Campbell, J. M. Cadogan, A. J. Studer, R. Zeng, and S. X. Dou, *Appl. Phys. Lett.* **98**, 232509 (2011).
- <sup>25</sup>C. F. Sánchez-Valdés, P. J. Ibarra-Gaytán, J. L. Sánchez Llamazares, M. Avalos-Borja, P. Álvarez-Alonso, P. Gorria, and J. A. Blanco, *Appl. Phys. Lett.* **104**, 212401 (2014).
- <sup>26</sup>P. Álvarez-Alonso, J. L. Sánchez Llamazares, C. F. Sánchez-Valdés, G. J. Cuello, V. Franco, P. Gorria, and J. A. Blanco, *J. Appl. Phys.* **115**, 17A929 (2014).